



EFFECT OF VIBRATIONS ON FRACTURE PHENOMENA IN MACHINING ARAMID-GLASS FIBER HYBRID COMPOSITES

E. NAKANISHI, J. SUZUKI and K. ISOGIMI

DEPARTMENT OF MECHANICAL ENGINEERING, FACULTY OF ENGINEERING,
MIE UNIVERSITY,

Kamihama-cho 1515, Tsu, 514-8507, Mie, JAPAN

Machining of A-GFRP is needed to provide desired shapes, but involves many problems such as the drop of the surface integrity of the materials due to fluffing of the fibers. The ultrasonic vibration has been applied to the cutting tool during machining. The aramid-glass hybrid FRP consists of four layers of hybrid roving cloth and five layers of chopped strand glass mats, and a polyester resin as the matrix. This FRP has very poor machinability resulting from the presence of aramid fibers. The wear of the cutting tool and roughness of the machined surface are measured, and cutting phenomena are investigated by a comparison with normal cutting conditions.

Key Words: Aramid fiber, Microscopic observation, Vibrational cutting, Tool wear, Surface appearance

1. EXPERIMENTAL PROCEDURES

A-GFRP (aramid-glass hybrid FRP) has been chosen as the material. This hybrid material has low machinability caused by aramid fibers. A-GFRP used in this research is shown in Fig. 1 and consists of four layers of hybrid cloth and five layers of chopped strand mats of glass fibers, with the matrix being made of polyester. Each piece of hybrid cloth is woven of long fibers of aramid and glass. The thickness of A-GFRP composite is about 10 mm, and it is machined into a circular disk of about 150 mm in diameter using a lathe. These disk-type A-GFRPs are machined orthogonally by normal and vibrational cutting with a feed rate of 0.05mm/rev. Ultrasonic vibration is used for orthogonal cutting. Cutting by ultrasonic vibration will stop if the maximum speed of the vibrating tool is larger than that of the workpiece. Figure 2 shows vibrational cutting equipment in detail. The cutting tool (WC cutting tool) is affixed to the top of the horn, which is connected firmly to the ultrasonic oscillator. In addition, the horn is supported on the tool post of the lathe at the node position of the vibration.

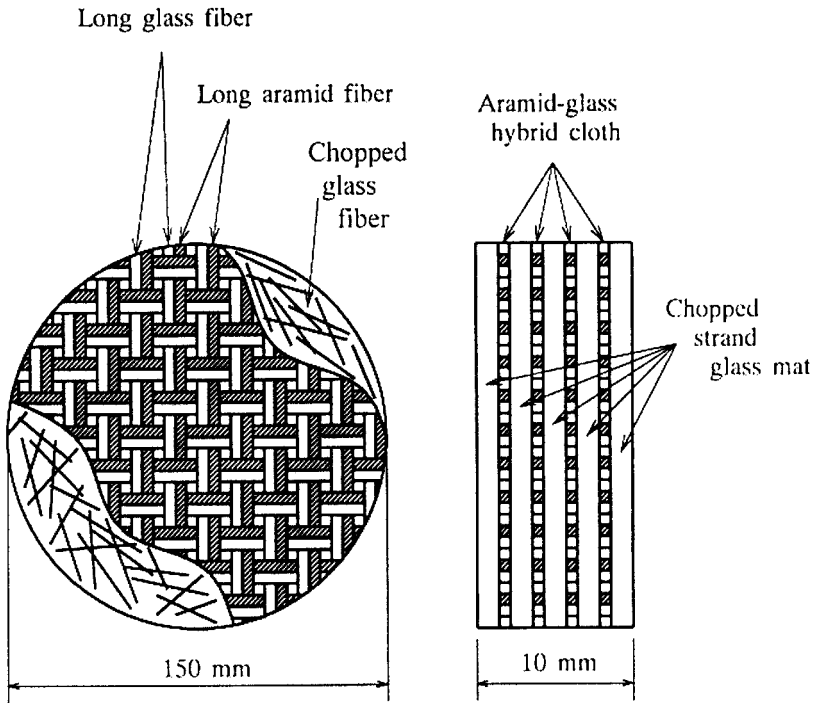


FIG. 1. Construction of aramid-glass FRP.

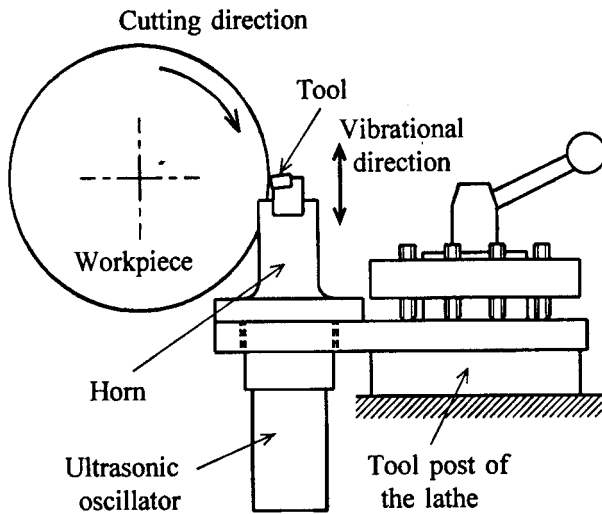


FIG. 2. Experimental setup.

2. VIBRATIONAL CUTTING

The most important point in adding ultrasonic vibration to the cutting tool is to detach the tool edge periodically from the workpiece at each vibration cycle. Therefore, cutting speed v should be selected so as to be smaller than the retreating speed of the tool edge (critical speed to interrupted cutting v_c). The relative behavior of tool edge to the workpiece is considered from the view-point of the cutting speed. The period of the cutting stage (contact period with the work), displacement of the tool edge and relative cutting speed v are changed considerably during each vibrating cycle by the conditions of vibration and work motion. Therefore, the effects of adding ultrasonic vibration can be expected to be very effective. It is supposed that the motion of the vibrating tool is expressed by the following trigonometric function, as shown in Fig. 3(a),

$$(2.1) \quad y = a \sin(2\pi ft)$$

where y is the position or displacement of the tool edge from the center of the ultrasonic vibration, a is the half-width of the amplitude, f is the frequency of the vibration and t is the time in seconds. In this experiment, a is $15 \mu\text{m}$ and f is 20 kHz. Thus, the velocity of the tool edge v_e is given as follows:

$$(2.2) \quad v_e = \frac{dy}{dt} = 2\pi fa \cos(2\pi ft).$$

The cutting speed, v_r , is the relative speed of the tool edge to the workpiece surface. That is,

$$(2.3) \quad v_r = v_e - v = 2\pi fa \cos(2\pi ft) - v$$

where v is the tangential speed of the workpiece. Figure 3(b) shows the change in v during the cutting process. This research is performed under the conditions of cutting speeds or tangential speed of the workpiece being $v = 28.3, 84.8, 169.9 \text{ m/min}$. The surface of the workpiece moves downwards at the position contacting the tool edge. The straight line in Fig. 3(a) shows the position of the cutting location on the workpiece moving with a tangential speed of 28.3 m/min .

At $t = 0$, cutting is performed at a maximum cutting speed of $2\pi fa - v$. Actual cutting is kept during the period when v_r is positive. If the retreating speed of the tool edge is reduced to zero and becomes negative, cutting is stopped and then, the cutting edge separates from the workpiece. Time t_1 , when cutting stops, is obtained from Eq. (2.3) by substituting $v_r = 0$. That is,

$$(2.4) \quad t_1 = \frac{1}{2\pi f} \cos^{-1} \frac{v_e}{2\pi fa}.$$

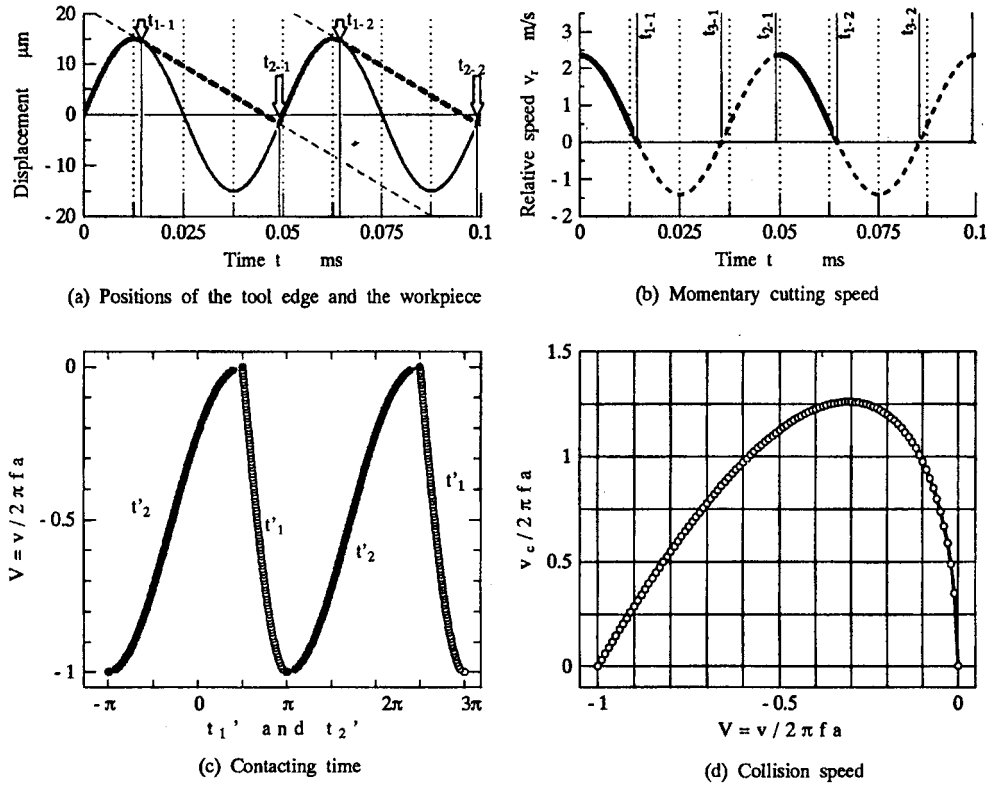


FIG. 3. Relative behavior of tool edge to workpiece during vibrational cutting.

Cutting is discontinuous under the condition of $|v| < |2\pi fa|$ and is continuous under that of $|v| > |2\pi fa|$. Although cutting is continuous, cutting speed v is changed by applying vibration during each vibration cycle. The critical speed of workpiece surface, v_c , to the interrupted cutting is obtained from $|v| = |2\pi fa|$. For these experiments, $v_c = 113$ m/min.

Even if v_r increases and becomes positive, cutting does not start again immediately because of the edge separation of the tool from the workpiece. Time t_2 , when the cutting re-starts, satisfies the following equation:

$$(2.5) \quad \int_{t_1}^{t_2} v_r dt = \int_{t_1}^{t_2} (v_e - v) dt = 0.$$

That is,

$$(2.6) \quad \sin(2\pi ft_2) - \sin(2\pi ft_1) = \frac{v}{a}(t_2 - t_1).$$

The value of time t_2 can not be determined analytically. Therefore, two parameters have been introduced to characterize the properties of vibrational cutting,

that is, non-dimensionalized vibrational cutting speed $V = v/(2\pi fa)$, and non-dimensional time $t' = 2\pi ft$. Two Eqs. (2.4) and (2.6) can be rewritten using parameters V and t' :

$$(2.7) \quad t'_1 = \cos^{-1} V,$$

$$(2.8) \quad \sin t'_2 - \sin t'_1 = V(t'_2 - t'_1).$$

Figure 3(c) shows t'_1 and t'_2 which have been calculated by the numerical method. The speed of collision between the edge and the workpiece, v_r , when the cutting restarts, is obtained by substituting t'_2 into Eq.(2.3). The value of v_r is shown in Fig. 3(d). The speed of collision v_r becomes maximum at a vibrational cutting speed V of about 0.3. The values of V for this experiments are listed in Table 1.

Table 1. Nondimensional cutting speed V .

v m/min	V
28.3	0.25
169.6	1.50

3. SURFACE APPEARANCE

Figure 4 shows the effect of the adding ultrasonic vibration on the machined surface appearance under the condition of cutting speed $v = 23.9$ m/min. The aramid fibers are elongated and compressed strongly on the surface of the specimen, and long and wide fluffs appear on the machined surface during cutting with no vibration(normal cutting). However, cutting with ultrasonic vibration improves the surface appearance of the machined surface. Long and wide fluffs rarely appear in the hybrid bundle region compared with other cutting methods. Therefore, it is thought that this method may be able to create a desirable surface. The appearances of aramid fibers on the machined surface is remarkably influenced by the orientation of the fibers. In this work, the material is machined by a lathe, therefore, fiber angle θ is changed continuously along the circumferential surface of the disk material. Angle θ is defined and illustrated in the above photos in Fig. 4. When angle θ is smaller than the right angle, the fibers will be lifted up by the tool edge from the machined surface of the matrix. The aramid fibers that have been lifted are not supported by the matrix, so the tool edge is not able to cut them properly under normal cutting conditions. As a result, long fluffs of aramid fibers could be observed. However, when angle θ is greater than the right angle, for example, $\theta = 135$ degree, fibers will be compressed strongly

between the tool edge and the matrix. Aramid fibers are deformed by the forward cutting force, and it can be observed that the fibers resemble fish scales on the surface. This cutting mechanism has been named “ironing” by J.E.D. AFAGHANI *et. al.* [1].

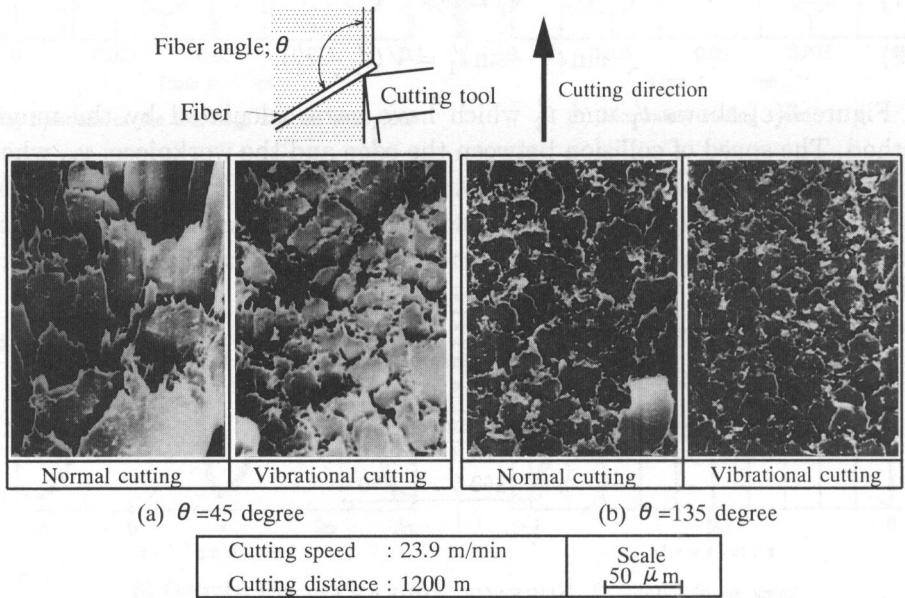


FIG. 4. Examples of the surface appearance of the machined surface.

We can notice that the size of fluff increases as fiber angle θ decreases. The long fluffs of the aramid hybrid appear on the machined surface during normal cutting, at the time when the tool remains in contact with the workpiece through the cutting process. Here, it is considered that the tool advances continually compressing forward and downward at the same time rather than extending the aramid fiber, then finally aramid fiber is torn away by the bending tensile force at the curved cutting edge. Therefore, long fluffs appear on the machined surface under normal cutting. Due to small elongation of the aramid fiber, the tensile force does not play any essential part in creating long fluffs during cutting. During vibrational cutting, similar phenomena always occur. However, due to the widely changing relative cutting speed and the presence of high-speed collision between the tool edge and the fibers by adding ultrasonic vibration, the fiber will be able to be cut easily. Further, in the interrupted cutting operation the cutting tool repeats separation from the workpiece and collision with the fibers in each vibrating cycle, therefore, the aramid fiber is not pulled continually by the tool edge during machining. So the resultant fluffs become shorter than those due to normal cutting.

4. SURFACE ROUGHNESS

Maximum roughness of the machined surface integrity R_y are measured to evaluate surface in comparison with the normal-type cutting. Figure 5 shows that the surface roughness of the A-GFRP specimen decreases with an increase in fiber angle θ when θ is greater than 45 degrees. These results are evident from the fact that the fluffs in the surface region raise and become longer at lower θ , as described in Fig. 4. The R_y increases considerably with the increment of the cutting speed. Vibrational cutting is effective when the cutting speed exceeds the critical one.

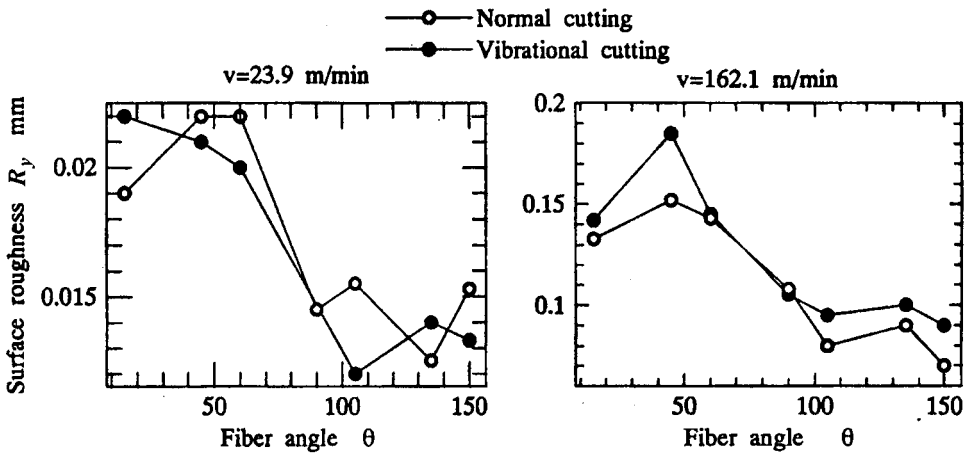


FIG. 5. Effect of fiber angle θ on surface roughness.

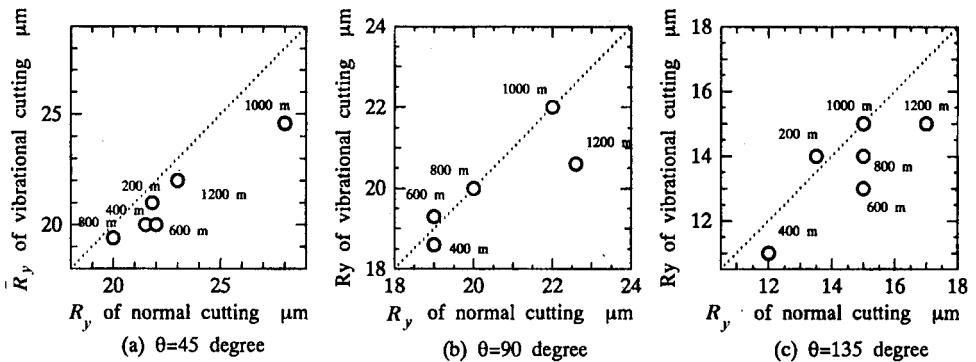


FIG. 6. Improvement of tool wear with ultrasonic vibration ($v = 23.9$ m/min).

Figure 6 shows surface roughness R_y by adding ultrasonic vibration plotted against the value of normal cutting. As both values of R_y for normal and vibrational cutting are plotted along X and Y axis of the figure, so these figures

show that the vibrational cutting is effective in the region under the diagonal line. Figures 6 (a)~(c) show values of R_y in the cases of fiber angle θ of 45, 90 and 135 degrees, respectively. The useful effect of adding ultrasonic vibration is recognized at a fiber angle of $\theta = 45$.

5. TOOL WEAR

The cutting tool was worn out, as shown schematically in Fig. 7. It could be observed that there were four large wear regions in the flank of the tool, corresponding to the position of aramid glass hybrid cloth layers. The three kinds of wear values were measured, that is, the maximum width of the flank wear VB_{max} and the mean width of flank wear band VB and face wear width KB .

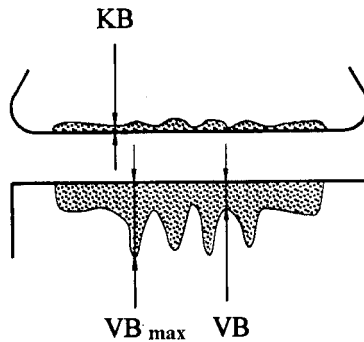


FIG. 7. Illustration of tool wear.

Figure 8 shows an example of the development of the flank wear width VB_{max} compared with cutting distance L concerning the ultrasonic vibration and the normal one. These results are derived in cutting A-GFRP composite at a cutting speed of $v = 28.3$ and 169.6 m/min. In the early stage of the cutting distance (shorter than 50 m), the effect of adding ultrasonic vibration fails to occur. Also, flank wear width VB_{max} increases steeply. As cutting distance L increases, vibrational cutting is effective when the cutting speed is $v = 169.6$ m/min.

The effect of adding ultrasonic vibration does not appear clearly. However, vibrational cutting is effective as cutting distance L increases. Figure 8 shows the tool wear adding ultrasonic vibration plotted against the values of normal cutting. Figures 9 (a)~(c) show VB_{max} , VB and KB , respectively. Tool wear increases with the cutting distance and the tool wears are decreased by adding the ultrasonic vibration in each case. At the interrupted cutting, tool edge does not remain in contact with the workpiece during the cutting process, so there is a lesser contact period of the tool-work interface the less wear width. The effect

of vibration is the greatest in KB and small in VB_{\max} . However, the reduction rate of wear is between 11~16 %.

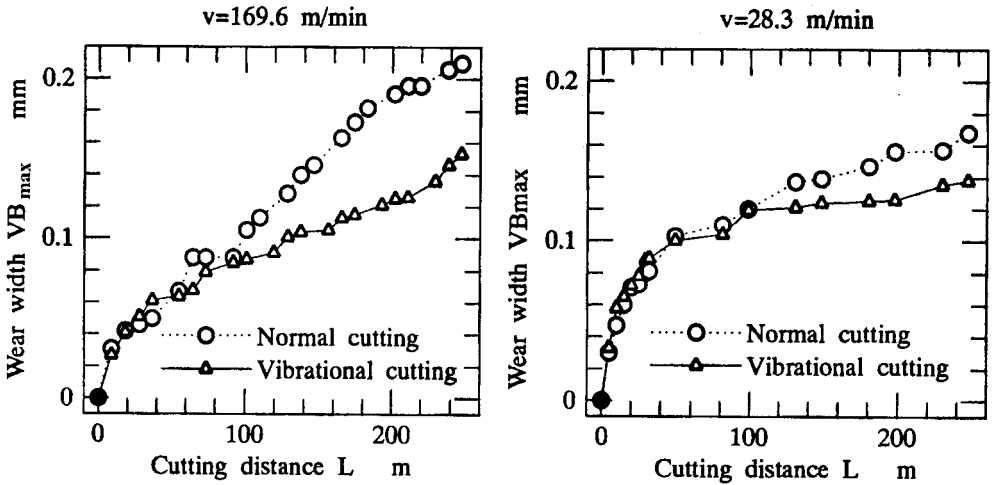


FIG. 8. Development of flank wear width VB_{\max} .

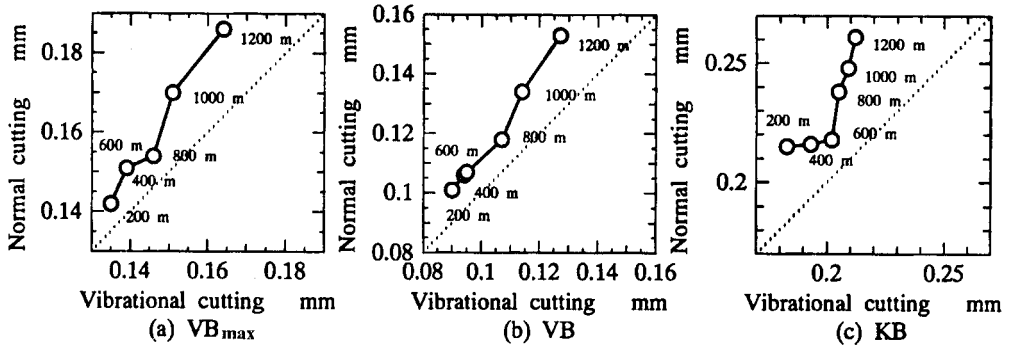
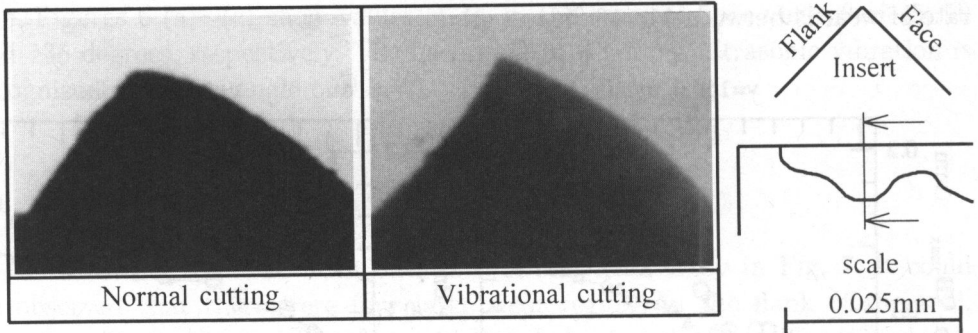


FIG. 9. Improvement of surface roughness with ultrasonic vibration ($v = 23.9$ m/min).

Figure 10 shows the photos of the cross-section of the tool edges worn by cutting the hybrid cloth. The retainment of the sharpness of the tool edge is comparatively better for ultrasonic vibration cutting. Due to interrupted cutting, there is a non-cutting period and it is reported that the interrupted cutting reduces the cutting force compared with that of the normal cutting. The sharpness of the edge may cause superior surface integrity.



Cutting speed : 23.9 m/min

Cutting distance : 1200 m

FIG. 10. Cross-sectional views of the edges.

6. CONCLUSIONS

Brief summary of the conclusions obtained:

1. The fluffs on the machined surface in vibrational cutting become shorter than those of normal cutting, without any relation to the directions of vibration.
2. Appearance of the machined surface can be improved by adding ultrasonic vibration to the cutting tool edge.
3. Tool wear always decreases with the addition of ultrasonic vibration. For example, at a cutting speed of $v = 169.6$ m/min, flank wear VB_{\max} decreases by about 20 ~ 30%.
4. The effectiveness of vibrational cutting also depends on the retainment of the sharpness of the tool edges .

REFERENCES

1. J.E.D. AFAGANI, K. ISOGIMI and J. SUZUKI, *Cutting of aramid fiber in A-GFRP composite*, Advancement of Intelligent Production, Elsevier Sc.B.V., 407-412, 1994.

Received November 30, 1998; revised version August 14, 1999.